Original article

Epileptic Disord 2012; 14 (4): 404-13

White matter abnormalities revealed by DTI correlate with interictal grey matter FDG-PET metabolism in focal childhood epilepsies

Sarah Lippé [1,2,3,9], Cyril Poupon [2,3], Arnaud Cachia [4], Frédérique Archambaud [1,10], Sébastian Rodrigo [1,2], Georg Dorfmuller [1,7], Catherine Chiron [1,2,3,8], Lucie Hertz-Pannier [1,2,3]

[1] INSERM U663, University Paris Descartes, Faculty of Medicine, Paris
[2] Service Hospitalier Frédéric Joliot, Orsay and NeuroSpin, I2BM, CEA, Saclay
[3] Institut Fédératif de Recherche IFR 49, Gif-sur-Yvette
[4] INSERM U894, Centre de Psychiatrie & Neurosciences, Paris
[5] Université Paris Descartes, Sorbonne Paris Cité, Paris
[6] CNRS U3521, Laboratoire de Psychologie du développement et de l'Education de l'Enfant, Paris
[7] Department of Neurosurgery, Fondation Ophtalmologique Rothschild, Paris
[8] AP-HP, Necker Hospital, Department of Neuropediatrics, Paris, France
[9] Département de psychologie, CHU Sainte-Justine, Université de Montréal, Canada
[10] Service Médecine Nucléaire, CHU Bicêtre, APHP, Université Paris-Sud

Received September 23, 2012; Accepted October 22, 2012

ABSTRACT – For patients with focal epilepsy scheduled for surgery, including MRI-negative cases, ^{18}FDG-PET was shown to disclose hypometabolism in the seizure onset zone. However, it is not clear whether grey matter hypometabolism is informative of the integrity of the surrounding white matter cerebral tissue. In order to study the relationship between metabolism of the seizure onset zone grey matter and the integrity of the surrounding white matter measured by diffusion tensor imaging (DTI), we performed a monocentric prospective study (from 2006 to 2009) in 15 children with pharmacoresistant focal epilepsy, suitable for interictal ^{18}FDG-PET, T1-, T2-, FLAIR sequence MRI and DTI. Children had either positive or negative MRI (eight with symptomatic and seven with cryptogenic epilepsies, respectively). Seven children subsequently underwent surgery. Standardised uptake values of grey matter PET metabolism were compared with DTI indices (fractional anisotropy [FA], apparent diffusion coefficient [ADC], parallel diffusion coefficient [PDC], and transverse diffusion coefficient [TDC]) in grey matter within the seizure onset zone and adjacent white matter, using regions of interest automatically drawn from individual sulcal and gyral parcellation. Hypometabolism correlated positively with white matter ADC, PDC, and TDC, and negatively with white matter FA.

Correspondence:
Sarah Lippé
CHU Sainte-Justine Research Center,
Psychology Department,
University of Montreal,
CP 6128, Succursale Centre-Ville,
Montréal, Québec,
H3C 3J7, Canada
<Sarah.lippe@umontreal.ca>

doi:10.1684/epd.2012.0547

In the cryptogenic group of children, hypometabolism correlated positively with white matter ADC. Our results demonstrate a relationship between abnormalities of grey matter metabolism in the seizure onset zone and adjacent white matter structural alterations in childhood focal epilepsies, even in cryptogenic epilepsy. This relationship supports the hypothesis that microstructural alterations of the white matter are related to epileptic networks and has potential implications for the evaluation of children with MRI-negative epilepsy.

Key words: FDG-PET, metabolism, white matter, epilepsy, network, DTI

Children with intractable partial epilepsy can be successfully treated by neurosurgery (Freitag and Tuxhorn, 2005; Wyllie *et al*., 2007; Delalande *et al*., 2007; Kim *et al*., 2008; Harvey *et al*., 2008; Hemb *et al*., 2010; Dunkley *et al*., 2011), but outcome is closely linked to precise delineation of the seizure onset zone (SOZ) (Paolicchi *et al*., 2000). To this end, presurgical investigation includes clinical ictal and interictal semiology, interictal and ictal scalp electroencephalography (EEG), structural imaging (high resolution T1-, T2-, fluid-attenuated inversion recovery [FLAIR]- magnetic resonance imaging [MRI] sequences), ^{18}F-fluorodeoxyglucose positron emission tomography (^{18}F-FDG PET), and in selected cases, intracerebral recording (Cross *et al*., 2006). Although interictal FDG-PET hypometabolism extends beyond the SOZ proper (Juhász *et al*., 2001; Chassoux *et al*., 2004), FDG-PET and MRI coregistration further delineates focal abnormalities (Salamon *et al*., 2008) and may help to avoid intracortical recordings in an increasing number of cases (Chassoux *et al*., 2010). However, it is estimated that imaging techniques fail to reveal lesions in 20% of intractable partial epileptic patients (Koepp and Woermann, 2005).

Diffusion MRI (DTI) is widely used to study the microstructure of the brain. Modelling the 3D displacement of water molecules within tissue components (Oppenheim *et al*., 2007) yields indices reflecting tissue structure. The apparent diffusion coefficient (ADC), transverse diffusion coefficient (TDC, $\lambda_{\perp}$), and parallel diffusion coefficient (PDC, $\lambda\|$) reflect the average displacement of free water molecules, either globally, perpendicular to (transverse) or along the (parallel) main diffusion axis, while fractional anisotropy (FA) reflects the directionality of the displacement (Adcock *et al*., 1998). In white matter (WM) neural fibres, intact membranes are the primary determinant of anisotropic water diffusion, whereas the relative degree of myelination is reflected more by radial diffusivity (Song *et al*., 2002) (Concha *et al*., 2006).

Diffusion abnormalities have previously been described in adult epileptic patients. In those with acquired or developmental lesions visible on MRI (symptomatic epilepsies), recent studies indicated 100% sensitivity of diffusion index changes, particularly ADC increase and FA decrease (Rugg-Gunn *et al*., 2001; Guye *et al*., 2007). These diffusion changes may reflect the lesion itself as well as epilepsy-related functional changes. Elevated ADCs have been found around the MRI-apparent lesion as well as remote locations (Rugg-Gunn *et al*., 2001; Thivard *et al*., 2006; Guye *et al*., 2007). In areas investigated by intracerebral electrode recordings, regions adjacent to visible focal cortical dysplasias (FCDs) with normal appearance showed elevated ADC values, with no change in FA (Thivard *et al*., 2006; Guye *et al*., 2007). In 20 to 33% of patients with negative MRI (cryptogenic epilepsies), which corresponds to cortical dysplasias in 50% of cases (Bautista *et al*., 2003), subjects showed an increase in ADC concordant with the SOZ (Rugg-Gunn *et al*., 2001; Guye *et al*., 2007). In some cases, diffusion changes also occurred beyond the SOZ, more often in regions highly structurally connected to the epileptogenic cortex. Moreover, ADC changes were associated with the duration of epilepsy (Guye *et al*., 2007). Among the rare studies in children, magnetoencephalographic (MEG) dipole clusters overlaying MRI-visible lesions were shown to match changes in both FA and ADC (Widjaja *et al*., 2009). Although the mechanisms underlying diffusion changes and their value in presurgical evaluation are not yet clear, studies strongly suggest the presence of tissue abnormalities within and beyond the MRI-visible lesion and/or SOZ. Authors suggest that distant tissue alterations are likely to reflect multifactorial structural changes (Guye *et al*., 2007; Rodrigo *et al*., 2007).

Interictal ^{18}F-FDG PET cost effectiveness in presurgical evaluation is well established (O'Brien *et al*., 2008). Focal cortical hypometabolism is found on simple visual inspection in most symptomatic cases and 42 to 78% of cryptogenic cases (Matheja *et al*., 2001; Lee *et al*., 2005; Chassoux *et al*., 2010). However, the significance of cortical hypometabolism in cryptogenic epilepsies is still debated. Some studies have failed to show a strong correlation with MRI signal changes or atrophy (O'Brien *et al*., 1997), topography of structural changes on MRI (Chassoux *et al*., 2004), or neuronal loss on resected specimens (Henry *et al*., 1994). But when compared to controls using statistical parametric mapping, FDG-PET interictal hypometabolism

in epileptic patients was shown to reflect not only the epileptogenic zone, but also the seizure spread (Chassoux *et al*., 2004). Recently, it was shown that PET-MRI co-registration can provide 95% sensitivity, in depicting Taylor-type dysplasia in adults, with good co-localisation of the epileptic zone and hypometabolism in 55% of cases (Chassoux *et al*., 2010).

Given both the very low metabolic level of WM and the limited spatial resolution that prevents a clear delineation between the cortex and the underlying WM, PET is not a suitable technique to test the integrity of the WM in areas adjacent to, or remotely located from the SOZ. In this study, we aimed to clarify the relationship between cortical hypometabolism and the microstructure of both grey matter (GM) and WM adjacent to the SOZ, by directly comparing FDG-PET and DTI in a series of 15 children awaiting surgery for pharmacoresistant partial epilepsy, either symptomatic (positive MRI) or cryptogenic (negative MRI). We hypothesized that cortical hypometabolism would be associated with microstructural disorganisation and/or cellular loss, detectable as an increase in diffusivity (ADC, TDC) and a decrease in anisotropy (FA) in the WM.

Methods

Patients

We performed a prospective study of children with focal epilepsy referred for presurgical FDG-PET investigation at the Frédéric Joliot Hospital, France, between December 2006 and February 2009. Patients were divided into two subgroups, depending on the presence or absence of lesions visible on MRI (T1-weighted, T2-weighted, and FLAIR sequences). Consent for biomedical research was obtained from parents of all participants and the project was accepted by the Ethics Committee of Paris Hospitals (France).

Of 50 consecutive children with non-syndromic intractable partial epilepsy identified for presurgical FDG-PET evaluation, 32 received all T1-weighted, T2-weighted, FLAIR, and DTI sequences. Seventeen were excluded due to movement artefacts on either PET (n=6) or diffusion imaging (n=11), despite sedation used for non-cooperative children. The remaining 15 children were included in the study: 8 had symptomatic epilepsy and 7 cryptogenic epilepsy (*table 1*). Mean age was 13.5 years and ranged from 11 to 16 years. The two subgroups did not differ according to clinical data: age (U=22.0, p=0.487), age at onset (Mann Withney's U=17.5, p=0.370), epilepsy duration (U=14.0, p=0.180), and seizure frequency (U=23.5, p=0.872).

Seven children subsequently proceeded to surgery (6 symptomatic, 1 cryptogenic). Histologically, 3 showed FCD (type IIA) including 1 case of cryptogenic epilepsy. Histopathology showed an ischaemic lesion, an astrocytic inclusion immunoresponsive to filamin A, a dysembryoplastic neuroepithelial tumour and a confirmed hippocampal sclerosis in the remaining 4 patients.

Image acquisition

MR images were acquired on a GE Signa 1.5T Excite II MRI system (General Electric, Milwaukee, WI, USA). High-resolution T1-weighted sequences were acquired by 3D inversion recovery fast gradient echo (slice thickness: 1.3 mm; field of view: 24 cm; matrix: $256 \times 256 \times 128$; TI/TE/TR: 600/2.0/9.9 ms). T2-weighted images were acquired by turbo spin-echo 3D sequence (180 slices; field of view: 250 mm; matrix: 250×250; TR: 2,500 ms; TE: 364 ms; Flip angle: 90 degrees). Parameters for the FLAIR sequence were: field of view: 230 mm; matrix size: 352×248; slice thickness: 5 mm; and TI/TR/TE: 2,800 ms/11,000 ms/125 ms. Diffusion MRI scanning was performed using a single-shot twice-refocused spin-echo EPI sequence (TE/TR: 66 ms/14 s; slice thickness: 2.5 mm; read bandwidth: 200 kHz; partial Fourier factor: 5/8; field of view: 24 cm; matrix: 128×128; 45 slices), with five T2-weighted images (b=0 s/mm^2) and 41 non-collinear directions uniformly distributed over the sphere (b=700 s/mm^2).

PET scans were performed using a high-resolution head-dedicated PET camera (Siemens ECAT EXACT HR+; 4.5 mm intrinsic resolution) with a field of view of 15.52 mm, providing 63 slices. Attenuation correction was performed using 68 Ge transmission scans acquired just before intravenous ^{18}F-FDG injection. A bolus of 0.37 MBq/kg (maximum dose: 148 MBq) ^{18}F-FDG was injected and dynamic images of 4 raw data sets of 5 minutes were acquired 30 minutes post-injection. Dynamic images were corrected for attenuation and summed into a 20-minute PET image used for processing.

Image preprocessing

FMRIB Software Library (FSL, www.fmrib.ox.ac.uk/fsl/) was used to correct DTI images for rigid head motion and eddy-current related distortions. We estimated ADC, PDC, TDC, and FA maps using the diffusion tensor model in BrainVISA software (www.brainvisa.info). Standard uptake values (SUV) with decay correction were calculated for each voxel of PET images and normalised by the mean metabolism of the cerebellum, as proposed by Ferrie *et al*. (1997). There was no focal hypometabolism nor hypermetabolism on visual inspection of the cerebellum. Our goal was to minimise potential confounding effects of inter-subject image variability on asymmetry indices. SUV was calculated by multiplying the glucose uptake values in each voxel by the body weight in kg, divided by the injected dose corrected for 30-minute decay.

Table 1. Clinical characteristics.

Epilepsy	Gender	Age (years)	Age at onset	Epilepsy Duration	Seizure frequency	Seizure onset Ictal EEG	Spikes at inter-ictal EEG	MRI lesion	PET hypometa-bolism	Consensus on seizure onset zone	Medication	Histology
Crypto	M	9.83	3 months	115 months	3	LSF	LF (***)	none	LFC	LSF	LVT	not operated (multifocal)
Crypto	M	11.08	3 years	103 months	3	PostC and Cent	LPostC	none	Lcent T	L PostCent	LTG, VPA	not operated
Crypto	F	14.25	6 years	93 months	3	LSPostC P	LPostC*	none	Lcent P	LPostC	CBZ, ESM	not operated
Crypto	F	16	13 years	37 months	3	LFOrb	LF	none	LF	LFOrb	OXC	not operated (language zone)
& Crypto	M	10.42	6 years	47 months	2	Llns	LFT	none	LTO	LT(T1)	LTG	not operated
Crypto	M	10.33	9 years	14 months	1	LFCent	Lprecent**	none	LF	Lpreeent	CBZ, OXC	not operated
Crypto	F	16.5	8 years	102 months	3	Lins	LFT**	none	Lcent	LpreC	VGB, OXC	Focal cortical dysplasia type IIA
Sympto	F	8.67	3 years	68 months	3	RST	RCentT (***)	RST (cort+subcort)	RST	RT (T1)	OXC CLB	Focal cortical dysplasia type IIB
Sympto	F	11	2 months	130 months	3	LT SO lat	LTO (***)	LInfTO	LTOP	LTO	OXC LVT	Focal cortical dysplasia type IIA
Sympto	F	14.85	2 years	144	3	LSF	LF* (***)	LSF(cort + subc)	LF C	LSF	CLB, LTG	Astrocytic inclusion immunoresponsive for filamin A
Sympto	M	11.5	$5^{1/2}$ years	72months	3	LO	LO** (***)	LO (corti +subcort)	LOP	LO	OXC	Ischemia
Sympto	F	15.58	12 years	43 months	1	LMedT	LT	LMedT (cort + subcort)	LT	LT (T4)	OXC LVT	not operated (seizure free)
Sympto	F	9.75	8,5 years	15 months	3	RT (T1, T2)	RFT ** (***)	RMedT (cort+subcort)	RT	RT(T1)	CBZ	Operation scheduled
Sympto	F	7.17	$5^{1/2}$ years	20 months	1	LMedT	LT**(***)	LMedT + amyg	Linf T P	LT (T2)	CBZ	not operated (no seizure at SEEG)
Sympto	F	12.25	8 years	49.6 months	1	LT	LT	LHippoSlecrosis	LT	LT (T1)	OXC, TPM	Hippocampal sclerosis

Seizure freq: 1. <1/month; 2. >1/month; 3. >1/day
* Subclinical; ** Bilateral propagation; (***)iEEG
L=left; S=superior; F=frontal; C=cingular; P=parietal; postC=postcentral; Cent=central; Lat=lateral; Cort=cortical; Amyg=amygdala; Ins=insula
R=right; Inf=inferior; T=temporal; O=occipital; CU=cuneus; preC=precentral; Orb=orbital; Med=medial; Subcort=subcortical; Hippo=hippocampus
LVT=Levetiracetam; CLB=Clobazam; LTG=Lamotrigine; CBZ=Carbamazepine; VPA=Valproic Acid; ESM=Ethosuximide; OXC=Oxcarbazepine; VGB=Vigabatrin

Image processing

As the study included children of various ages with different epilepsy-affected areas, the construct was not directly amenable to group comparisons. Instead, we designed a method that mimicked the clinical approach, comparing DTI and PET measures within WM and GM regions of ipsi- and contralateral hemispheres. First, T1-weighted images were segmented into GM, WM, and cerebrospinal fluid masks (Mangin *et al.*, 2004a, 2004b). Individual gyral GM regions of interest (ROIs) were extracted automatically using BrainVISA software and segmentation algorithms for sulci (Mangin *et al.*, 2004b) and gyri (Cachia *et al.*, 2003) (*figure 1A*). The gyral GM ROIs (mean volume: 20821.37±7512.07 mm^3) were then used to parcel the underlying WM into a geodesic Voronoi diagram (*figure 1B*).

The b=0 and T1 images were then aligned using a rigid 3D transformation, applicable also to FA, ADC, PDC, and TDC maps. We estimated another rigid 3D transform by coregistering PET and T1 images. Mean ADC, PDC, TDC, and FA were calculated in each WM ROI and SUVs were then calculated in each GM ROI.

Analyses were performed on an ROI involved in the epileptic zone and an ROI not involved in the epileptic zone. For each patient, one gyral GM ROI along with its underlying WM ROI, not encompassing the SOZ or related to SOZ areas, was identified. The ROI chosen was the superior frontal gyrus in 13 patients and the superior parietal gyrus (superior parietal lobule) in the remaining 2 patients. Subsequently, for each patient, gyral GM ROI along with the respective underlying WM ROI, encompassing the SOZ, was chosen. The SOZ was identified by a panel which included an epileptologist, neurophysiologist, neuroradiologist and neurosurgeon, based on ictal video-EEG recordings of scalp EEG of all patients and also depth electrodes in 8 patients. PET metabolism was assessed by a nuclear medicine physician in the context of clinical evaluations, using PET-MRI coregistration. Thus, the nuclear medicine physician was informed of clinical data. Hypometabolism could encompass more than one ROI in some patients, but without difference between symptomatic and cryptogenic patients. The level of hypometabolism considered to represent the SOZ in each patient did

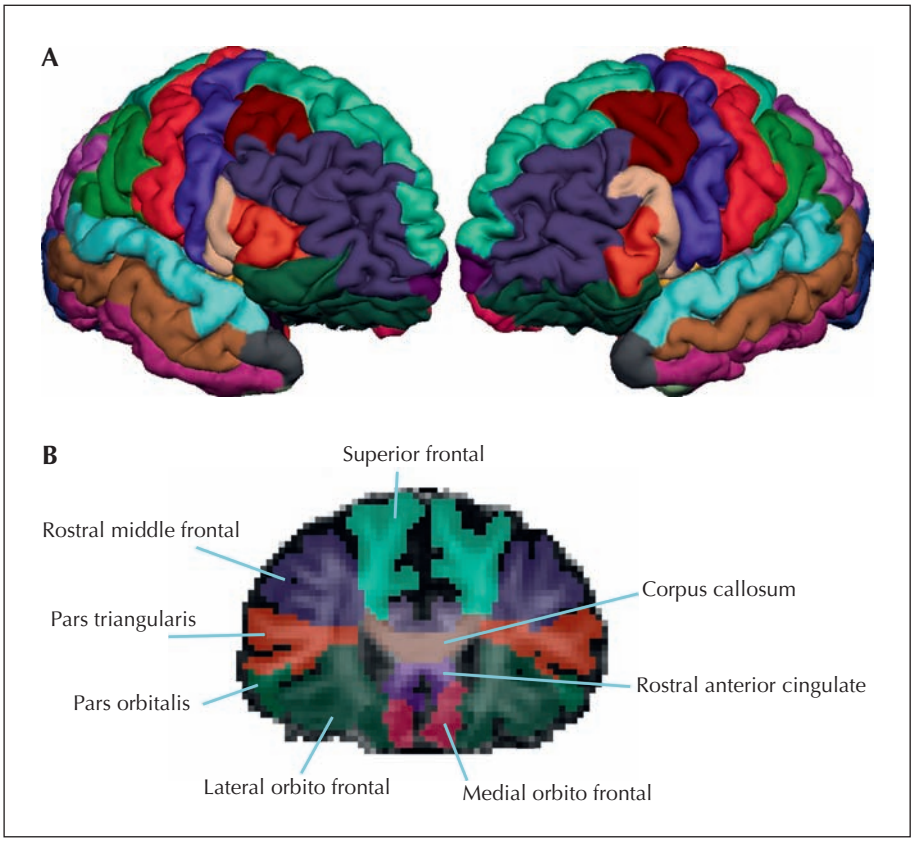

Figure 1. (A) Colour-coded individual gyral GM regions of interest (ROIs), extracted automatically using BrainVISA software. (B) GM ROIs and WM ROI co-registered on FA map.
Asymmetry index was calculated using homologue ipsilateral and controlateral hemispheres ROIs.

not always correspond to the highest level in the brain, but was considered the most clinically relevant according to the converging clinical and electrophysiological data. Interictal EEG, FDG-PET hypometabolism, and lesion on MRI (if any) provided additional arguments leading to a consensus for localising the SOZ. Asymmetry indices (AI) for mean SUVs, FA, ADC, PDC, and TDC were then calculated using ipsilateral and contralateral ROIs, as follows: (ipsilateral-contralateral)/(ipsilateral+contralateral). ROI volumes did not differ between ipsi- and contralateral sides (paired t-test; t=-1.73; dll=14; p=0.106). This intra-subject normalisation procedure allowed us to adjust for age, SOZ localisation, history of epilepsy and medications that could affect glucose uptake (Theodore *et al*., 1986; Theodore *et al*., 1989; Leiderman *et al*., 1991). Accordingly, the deeper the hypometabolism in the SOZ, the more negative the asymmetry index; similarly, the more reduced the FA, the more negative the index; and the higher the ADC, PDC, or TDC, the higher the index.

Statistical analyses

Statistical analyses were performed using SPSS software. Non-parametric correlations (Kendall's Tau-B) were performed for asymmetry indices (FDG-PET standard uptake values in the GM and FA, ADC, TDC, and PDC in the WM) and clinical data (age, age at onset, epilepsy duration and seizure frequency) for the total sample and subgroups separately (symptomatic, cryptogenic and temporal *vs* extratemporal).

Results

Initially, the analyses of clinical data were performed. Analyses were performed on the whole population tested, and subsequently, on individual groups. We found no correlation between metabolism or diffusion asymmetry indices and clinical data (age, epilepsy duration, seizure frequency, and age at onset).

Taking all children together, significant correlations were found between GM metabolism and diffusion asymmetry indices of WM ROIs corresponding to the SOZs (*figure 2 and table 2*). GM metabolism correlated negatively with WM ADC, PDC, and TDC and positively with WM FA (*table 2*).

No correlations were found between GM metabolism and diffusion asymmetry indices of WM control ROI (p>0.062).

In the symptomatic group, GM metabolism correlated positively with FA. In the cryptogenic group, GM metabolism correlated negatively with ADC (*table 2*). No correlations were found between GM metabolism and diffusion asymmetry indices of WM control ROI for each group, separately. Finally, diffusivity

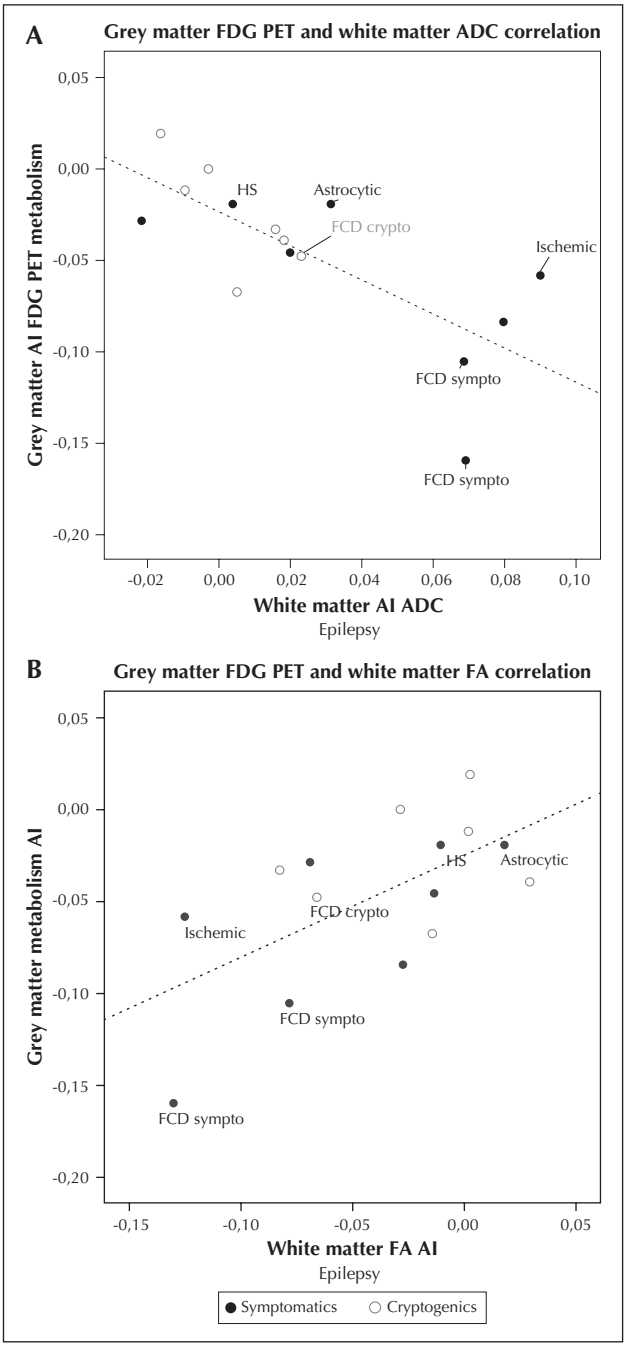

Figure 2. (A) White matter apparent diffusion coefficient asymmetry index correlates negatively with grey matter FDG-PET metabolism asymmetry index (r=-0.581, p=0.003). (B) White matter fractional anisotropy (FA) asymmetry index correlates with grey matter FDG-PET metabolism asymmetry index (r=0.448, p=0.020).

Full circles correspond to symptomatic epilepsy whereas empty circles correspond to cryptogenic epilepsy. Cases with histological results are labelled. The patient with positive metabolism AI is identified by & in *table 1*. Positive metabolism AI in this patient could be due to the size of the ROI, in contrast to the size of the hypometabolic area.

ADC: apparent diffusion coefficient; FDC: focal cortical dysplasia; HS: hippocampal sclerosis; astrocytic: astrocytic inclusion immunoresponsive to filamin A.

Table 2. Correlations between metabolism and diffusion indices.

Grey matter metabolism			
	All subjects	**Symptomatic**	**Cryptogenic**
Diffusion Index	r values/*p* values		
FA	**0.448/0.02	**0.714/0.013	0.143/0.652
ADC	** -0.581/0.003	-0.357/0.216	*-0.619/0.051
PDC	** -0.440/0.023	-0.357/0.216	-0.195/0.543
TDC	** -0.448/0.02	-0.500/0.083	-0.429/0.176

**< 0.05; *=0.051; FA: fractional anisotropy; ADC: apparent diffusion coefficient; PDC: parallel diffusion coefficient; TDC: transverse diffusion coefficient.

asymmetry indices of WM SOZ ROIs were compared between patients with TLE (*n*=7) and extraTLE (*n*=8). No significant results were found ($p>0.05$).

Discussion

In this study, metabolism in the SOZ was negatively correlated with diffusion indices ADC, PDC, and TDC and positively correlated with FA in the adjacent WM. Interestingly, such relationships were found not only in children with visible lesions, but also in children with cryptogenic epilepsy, where SOZ GM hypometabolism correlated with subjacent WM ADC. The absence of significant results in the cryptogenic group between GM metabolism and WM FA may result from the fact that cryptogenic patients have subtle lesions which are difficult to locate, possibly making it more difficult to define the epileptogenic zone. Another possibility could be the variability of underlying lesions, with different effects on movement/direction of water molecules. In symptomatic patients, the lesion may add to abnormalities related to the epileptic network.

In epileptic patients, most FDG-PET scans show alterations in GM, reflecting abnormal activity in cell bodies and synapses. Glucose uptake is disrupted not only in SOZs but also in remote cortical areas of the epileptic network (Juhász *et al*., 2002). However, on searching for remote GM structural abnormalities in children with temporal lobe epilepsy, Kimiwada *et al*. (2006) found no correlation between FDG-PET hypometabolism and DTI measures in deep GM structures (hippocampus, thalamus, and lentiform nucleus). In children with tuberous sclerosis complex, subcortical WM with normal appearance surrounding the epileptogenic and hypometabolic tubers showed decreased FA and increased TDC (Widjaja *et al*., 2010), suggesting the presence of microstructural alterations resulting from unknown mechanisms. Our study provides additional convincing evidence of the association between adjacent WM alteration and the SOZ cortical hypometabolism seen in PET scans, even when no lesion is visible in the SOZ. Specific correlation with the SOZ was suspected since no correlation was found in control ROI, which did not encompass known epilepsy tissue. Consequently, it would appear to be useful to investigate WM abnormalities with DTI during surgical evaluation, even when MRI is normal.

The link between WM abnormalities and EEG paroxysmal activity is unclear. Reduced FA and increased TDC in WM are correlated with severity of spike-and-wave discharges in a rat model of absence seizure (Chahboune *et al*., 2009). The authors speculated that chronic seizures cause WM alterations in what had previously been considered a predominantly GM disease. In our study, SOZ GM metabolism and WM ADC were correlated, even in the cryptogenic group. Increased ADC is reported to be responsive to seizures and induction of status epilepticus (Zhong *et al*., 1993; Ebisu *et al*., 1996; Wieshmann *et al*., 1997), reflecting cellular swelling and a reduction of extracellular space. However, our results are unlikely to be related to seizure occurrence since our patients were seizure-free for at least 12 hours preceding image acquisition. Nonetheless, our study did not reveal any correlation between either PET or DTI measures and seizure frequency, epilepsy duration and age at onset. The latter could be related to our small sample size.

Both hypometabolism and WM ADC changes might reflect microscopic tissue alteration, undetectable on standard MRI. In children and adults, FCD is frequently overlooked (Salamon *et al*., 2008; Besson *et al*., 2008). Indeed, as far back as 1971, Taylor *et al*. had suggested that cryptogenic epilepsies were caused by underlying lesions, describing giant glial cells in the layers beneath affected cortex and in the subjacent WM of seemingly normal cortical tissue. In those instances, increased ADC in the WM could reflect disturbed development resulting in reduced membrane density.

In the present study, histopathology was available for only 7 patients, limiting analysis to qualitative descriptions. In symptomatic patients, our results corroborate previous findings found in GM and WM on both MRI (T2-weighted and FLAIR) and DTI (Eriksson *et al*., 2001; Rugg-Gunn *et al*., 2001; Gross *et al*., 2006; Guye *et al*., 2007). Interestingly, the one child previously characterised as cryptogenic (*figure 2*), but showing a FCD on histology, revealed important changes in both DTI values and FDG-PET GM metabolism. We observed an expected reduced anisotropy and increased diffusivity in the SOZ. The last operated patient showed hippocampal sclerosis and increased

ADC in the hippocampus and surrounding temporal WM, as previously reported in adults (Thivard *et al*., 2005; Parmar *et al*., 2006).

The symptomatic group showed MRI findings pointing to abnormalities in adjacent WM. As previously reported (Song *et al*., 2002; Fink *et al*., 2010), WM alteration was associated with decreased FA and a tendency towards increased TDC, evoking changes in fibre orientation, density and myelination (Drobyshevsky *et al*., 2005; Snook *et al*., 2005), in addition to the presence of abnormal cells in the WM. Indeed, myelin-deficient mice and rats with a mutation of the gene for myelin basic protein showed decreased anisotropy of up to 25% (Gulani *et al*., 2001; Song *et al*., 2002). TDC has been shown to reflect the degree of myelination in healthy infants (Dubois *et al*., 2008). Developmental or ischaemic lesions are indeed accompanied by altered fibre organisation and myelination.

In the present study, we used an automated method to search for subtle changes in individual brains, by comparing both hemispheres quantitatively. We showed possible specificity of the measure in epileptic networks since no correlation between AI was found in a control ROI. However, this should be replicated and tested in surrounding ROIs of hypometabolism before drawing clear conclusions. While we used a conventional DTI sequence with a low b value (700) at 1.5T, we were able to highlight microstructural anomalies in adjacent WM epileptic networks, even for cryptogenic epilepsies. Such a method may therefore provide additional information in the presurgical work-up of epilepsy in the future. This study opens up the possibility of a more powerful, substantiated diagnosis of epileptogenic areas by DTI, using higher magnetic fields (3T and more), stronger diffusion gradients ($b>1,500$ sec/mm^2) and more elaborate diffusion models (such as high angular resolution diffusion imaging).

The first limitation of our study is the heterogeneity of localisation of the SOZ between children. It is unknown how the lobar localisation of the SOZ (*i.e*. temporal *vs* extra-temporal epilepsies) may have influenced our results. Depending on the location of epilepsy, involved brain network and underlying pathology, the link between metabolism and adjacent WM microstructure may vary. Recent findings suggest that TLE patients with hippocampal sclerosis show more pronounced and extensive ADC abnormalities compared to controls and TLE patients without hippocampal sclerosis (Shon *et al*., 2010). The fornix and cingulum anisotropy are affected only in TLE with hippocampal sclerosis (Concha *et al*., 2009). However, in TLE without hippocampal sclerosis, frontal and temporal components of the corpus callosum, as well as the external capsule, showed reduced anisotropy, also suggesting extended epileptic networks (Concha *et al*., 2009). In our series, 8 patients had an extra-temporal lobe SOZ and 7 a temporal lobe SOZ, with only 1 case of confirmed hippocampal sclerosis. Accordingly, no significant differences were found when comparing FA, ADC, TDC, and PDC AI, nor absolute values in the SOZ between TLE and extra-TLE patients. Since only the adjacent WM area was investigated, abnormalities in extended regions of the brain may have been overlooked.

Another limitation is the small sample size. Childhood MRI studies are known to be difficult to perform since subjects are required to be patient, calm, and to remain still during MRI. Since this study was performed in the context of presurgical evaluation in children, DTI acquisition was not successfully completed for some children due to the length of time of the procedure. This may have biased our results since children showing behavioural difficulties may also have had more severe symptomatic or cryptogenic epilepsies. A larger group of symptomatic and cryptogenic children would have yielded more data. Furthermore, the lack of control group did not permit individual analyses. Individual analyses may have helped in targeting circumscribed regions of anomalies. However, we used a laterality index, whereby the contralateral side was considered as an internal control for each individual, in order to minimise confounding inter-individual variability of DTI metrics which is present even in the normal population. In contrast, lobar mean diffusivity is very similar in homologous regions of the right and left hemisphere in the normal population, except for the temporal lobe where the right temporal lobe shows higher mean diffusivity values (Yoshiura *et al*., 2010). Only 2 right temporal lobectomy patients were included in our series. Future multicentre studies are needed to address the relationship between cortical SOZ metabolism and structural imaging of the epileptogenic network. □

Acknowledgements and disclosures.

Sarah Lippé was supported by the Canadian Institutes of Health Research. Arnaud Cachia was supported by the Fondation Pierre Deniker. The authors are grateful to Drs Christine Bulteau and Martine Fohlen who followed the patients before surgery at the Fondation Rothschild, Paris, and to our medical editor, Danielle Buch, for revision of the manuscript.

None of the authors has any conflict of interest to disclose.

References

Adcock LM, Moore PJ, Schlesinger AE, Armstrong DL. Correlation of ultrasound with postmortem neuropathologic studies in neonates. *Pediatr Neurol* 1998; 19: 263-71.

Bautista JF, Foldvary-Schaefer N, Bingaman WE, Lüders HO. Focal cortical dysplasia and intractable epilepsy in adults: clinicalm, EEG, imaging, and surgical features. *Epilepsy Res* 2003; 55: 131-6.

Besson P, Andermann F, Dubeau F, Bernasconi A. Small focal cortical dysplasia lesions are located at the bottom of a deep sulcus. *Brain* 2008; 131: 3246-55.

Cachia A, Mangin JF, Rivière D, *et al*. A generic framework for the parcellation of the cortical surface into gyri using geodesic Voronoi diagrams. *Med Image Anal* 2003; 7: 403-16.

Chahboune H, Mishra AM, DeSalvo MN, *et al*. DTI abnormalities in anterior corpus callosum of rats with spike-wave epilepsy. *Neuroimage* 2009; 47: 459-66.

Chassoux F, Semah F, Bouilleret V, *et al*. Metabolic changes and electro-clinical patterns in mesio-temporal lobe epilepsy: a correlative study. *Brain* 2004; 127: 164-74.

Chassoux F, Rodrigo S, Semah F, *et al*. FDG-PET improves surgical outcome in negative MRI Taylor-type focal cortical dysplasias. *Neurology* 2010; 75: 2168-75.

Concha L, Gross DW, Wheatley BM, Beaulieu C. Diffusion tensor imaging of time-dependent axonal and myelin degradation after corpus callosotomy in epilepsy patients. *Neuroimage* 2006; 32: 1090-9.

Concha L, Beaulieu C, Collins DL, Gross DW. White-matter diffusion abnormalities in temporal-lobe epilepsy with and without mesial temporal sclerosis. *J Neurol Neurosurg Psychiatry* 2009; 80: 312-9.

Cross JH, Jayakar P, Nordli D. Proposed criteria for referral and evaluation of children for epilepsy surgery: recommendations of the Subcommission for Pediatric Epilepsy Surgery. *Epilepsia* 2006; 47: 952-9.

Delalande O, Bulteau C, Dellatolas G, *et al*. Vertical parasagittal hemispherotomy: surgical procedures and clinical long-term outcomes in a population of 83 children. *Neurosurgery* 2007; 60: ONS19-32; discussion ONS32.

Drobyshevsky A, Song SK, Gamkrelidze G, *et al*. Developmental changes in diffusion anisotropy coincide with immature oligodendrocyte progression and maturation of compound action potential. *J Neurosci* 2005; 25: 5988-97.

Dubois J, Dehaene-Lambertz G, Soarès C, Cointepas Y, Le Bihan D, Hertz-Pannier L. Microstructural correlates of infant functional development: example of the visual pathways. *J Neurosci* 2008; 28: 1943-8.

Dunkley C, Kung J, Scott RC, *et al*. Epilepsy surgery in children under 3 years. *Epilepsy Res* 2011; 93: 96-106.

Ebisu T, Rooney WD, Graham SH, Mancuso A, Weiner MW, Maudsley AA. MR spectroscopic imaging and diffusion-weighted MRI for early detection of kainate-induced status epilepticus in the rat. *Magn Reson Med* 1996; 36: 821-8.

Eriksson SH, Rugg-Gunn FJ, Symms MR, Barker GJ, Duncan JS. Diffusion tensor imaging in patients with epilepsy and malformations of cortical development. *Brain* 2001; 124: 617-26.

Ferrie CD, Marsden PK, Maisey MN, Robinson RO. Cortical and subcortical glucose metabolism in childhood epileptic encephalopathies. *J Neurol Neurosurg Psychiatry* 1997; 63: 181-7.

Fink F, Klein J, Lanz M, *et al*. Comparison of diffusion tensor-based tractography and quantified brain atrophy for analyzing demyelination and axonal loss in MS. *J Neuroimaging* 2010; 20: 334-44.

Freitag H, Tuxhorn I. Cognitive function in preschool children after epilepsy surgery: rationale for early intervention. *Epilepsia* 2005; 46: 561-7.

Gross DW, Concha L, Beaulieu C. Extratemporal white matter abnormalities in mesial temporal lobe epilepsy demonstrated with diffusion tensor imaging. *Epilepsia* 2006; 47: 1360-3.

Gulani V, Webb AG, Duncan ID, Lauterbur PC. Apparent diffusion tensor measurements in myelin-deficient rat spinal cords. *Magn Reson Med* 2001; 45: 191-5.

Guye M, Ranjeva JP, Bartolomei F, *et al*. What is the significance of interictal water diffusion changes in frontal lobe epilepsies? *Neuroimage* 2007; 35: 28-37.

Harvey AS, Cross JH, Shinnar S, Mathern BW; ILAE Pediatric Epilepsy Surgery Survey Taskforce. Defining the spectrum of international practice in pediatric epilepsy surgery patients. *Epilepsia* 2008; 49: 146-55.

Hemb M, Velasco TR, Parnes MS, *et al*. Improved outcomes in pediatric epilepsy surgery: the UCLA experience, 1986-2008. *Neurology* 2010; 74: 1768-75.

Henry TR, Babb TL, Engel J Jr, Mazziotta JC, Phelps ME, Crandall PH. Hippocampal neuronal loss and regional hypometabolism in temporal lobe epilepsy. *Ann Neurol* 1994; 36: 925-7.

Juhász C, Chugani DC, Muzik O, *et al*. Relationship of flumazenil and glucose PET abnormalities to neocortical epilepsy surgery outcome. *Neurology* 2001; 56: 1650-8.

Juhász C, Chugani HT, Muzik O, Chugani DC. Hypotheses from functional neuroimaging studies. *Int Rev Neurobiol* 2002; 49: 37-55.

Kim SK, Wang KC, Hwang YS, *et al*. Epilepsy surgery in children: outcomes and complications. *J Neurosurg Pediatr* 2008; 1: 277-83.

Kimiwada T, Juhász C, Makki M, *et al*. Hippocampal and thalamic diffusion abnormalities in children with temporal lobe epilepsy. *Epilepsia* 2006; 47: 167-75.

Koepp MJ, Woermann FG. Imaging structure and function in refractory focal epilepsy. *Lancet Neurol* 2005; 4: 42-53.

Lee SK, Lee SY, Kim KK, Hong KS, Lee DS, Chung CK. Surgical outcome and prognostic factors of cryptogenic neocortical epilepsy. *Ann Neurol* 2005; 58: 525-32.

Leiderman DB, Balish M, Bromfield EB, Theodore WH. Effect of valproate on human cerebral glucose metabolism. *Epilepsia* 1991; 32: 417-22.

Mangin JF, Poupon F, Duchesnay E, *et al*. Brain morphometry using 3D moment invariants. *Med Image Anal* 2004a; 8: 187-96.

Mangin JF, Rivière D, Cachia A, *et al*. A framework to study the cortical folding patterns. *Neuroimage* 2004b; 23: S129-38.

Matheja P, Kuwert T, Lüdemann P, *et al*. Temporal hypometabolism at the onset of cryptogenic temporal lobe epilepsy. *Eur J Nucl Med* 2001; 28: 625-32.

O'Brien JT, Desmond P, Ames D, Schweitzer I, Tress B. Magnetic resonance imaging correlates of memory impairment in the healthy elderly: association with medial temporal lobe atrophy but not white matter lesions. *Int J Geriatr Psychiatry* 1997; 12: 369-74.

O'Brien TJ, Miles K, Ware R, Cook MJ, Binns DS, Hicks RJ. The cost-effective use of 18F-FDG PET in the presurgical evaluation of medically refractory focal epilepsy. *J Nucl Med* 2008; 49: 931-7.

Oppenheim C, Ducreux D, Rodrigo S, *et al*. Diffusion tensor imaging and tractography of the brain and spinal cord. *J Radiol* 2007; 88: 510-20.

Paolicchi JM, Jayakar P, Dean P, *et al*. Predictors of outcome in pediatric epilepsy surgery. *Neurology* 2000; 54: 642-7.

Parmar H, Lim SH, Tan NC, Lim CC. Acute symptomatic seizures and hippocampus damage: DWI and MRS findings. *Neurology* 2006; 66: 1732-5.

Rodrigo S, Oppenheim C, Chassoux F, *et al*. Uncinate fasciculus fiber tracking in mesial temporal lobe epilepsy. Initial findings. *Eur Radiol* 2007; 17: 1663-8.

Rugg-Gunn FJ, Eriksson SH, Symms MR, Barker GJ, Duncan JS. Diffusion tensor imaging of cryptogenic and acquired partial epilepsies. *Brain* 2001; 124: 627-36.

Salamon N, Kung J, Shaw SJ, *et al*. FDG-PET/MRI coregistration improves detection of cortical dysplasia in patients with epilepsy. *Neurology* 2008; 71: 1594-601.

Shon YM, Kim YI, Koo BB, *et al*. Group-specific regional white matter abnormality revealed in diffusion tensor imaging of medial temporal lobe epilepsy without hippocampal sclerosis. *Epilepsia* 2010; 51: 529-35.

Snook L, Paulson LA, Roy D, Phillips L, Beaulieu C. Diffusion tensor imaging of neurodevelopment in children and young adults. *Neuroimage* 2005; 26: 1164-73.

Song SK, Sun SW, Ramsbottom MJ, Chang C, Russell J, Cross AH. Dysmyelination revealed through MRI as increased radial (but unchanged axial) diffusion of water. *Neuroimage* 2002; 17: 1429-36.

Taylor DC, Falconer MA, Bruton CJ, Corselli JAN. Focal dysplasia of the cerebral cortex in epilepsy. *J Neurol Neurosurg Psychiatry* 1971; 34: 369-87. doi:10.1136/jnnp.34.4.369

Theodore WH, Bairamian D, Newmark ME, *et al*. Effect of phenytoin on human cerebral glucose metabolism. *J Cereb Blood Flow Metab* 1986; 6: 315-20.

Theodore WH, Bromfield E, Onorati L. The effect of carbamazepine on cerebral glucose metabolism. *Ann Neurol* 1989; 25: 516-20.

Thivard L, Lehéricy S, Krainik A, *et al*. Diffusion tensor imaging in medial temporal lobe epilepsy with hippocampal sclerosis. *Neuroimage* 2005; 28: 682-90.

Thivard L, Adam C, Hasboun D, *et al*. Interictal diffusion MRI in partial epilepsies explored with intracerebral electrodes. *Brain* 2006; 129: 375-85.

Widjaja E, Zarei Mahmoodabadi S, Otsubo H, *et al*. Subcortical alterations in tissue microstructure adjacent to focal cortical dysplasia: detection at diffusion-tensor MR imaging by using magnetoencephalographic dipole cluster localization. *Radiology* 2009; 251: 206-15.

Widjaja E, Simao G, Mahmoodabadi SZ, *et al*. Diffusion tensor imaging identifies changes in normal-appearing white matter within the epileptogenic zone in tuberous sclerosis complex. *Epilepsy Res* 2010; 89: 246-53.

Wieshmann UC, Symms MR, Shorvon SD. Diffusion changes in status epilepticus. *Lancet* 1997; 350: 493-4.

Wyllie E, Lachhwani DK, Gupta A, *et al*. Successful surgery for epilepsy due to early brain lesions despite generalized EEG findings. *Neurology* 2007; 69: 389-97.

Yoshiura T, Noguchi T, Hiwatashi A, *et al*. Intra- and interhemispheric variations of diffusivity in subcortical white matter in normal human brain. *Eur Radiol* 2010; 20: 227-33.

Zhong J, Petroff OA, Prichard JW, Gore JC. Changes in water diffusion and relaxation properties of rat cerebrum during status epilepticus. *Magn Reson Med* 1993; 30: 241-6.